C. R. Physique 15 (2014) 90–99

Contents lists available at ScienceDirect

Comptes Rendus Physique

www.sciencedirect.com

Quasicrystals / Quasicristaux

Frustration and defects in non-periodic solids

Frustration et défauts dans les solides non périodiques

Rémy Mosseri [a], Jean-François Sadoc [b]

[a] *Laboratoire de physique théorique de la matière condensée, université Pierre-et-Marie-Curie, CNRS UMR 7600, 4, place Jussieu, 75005 Paris, France*
[b] *Laboratoire de physique des solides, université Paris-Sud, CNRS UMR 8502, 91405 Orsay cedex, France*

ARTICLE INFO

Article history:
Available online 4 October 2013

Keywords:
Aperiodicity
Frustrations
Defects
Complex intermetallic phases

Mots-clés :
Périodicité
Frustrations
Défauts
Phases intermétalliques complexes

ABSTRACT

Geometrical frustration arises whenever a local preferred configuration (lower energy for atomic systems, or best packing for hard spheres) cannot be propagated throughout space without defects. A general approach, using unfrustrated templates defined in curved space, have been previously applied to analyse a large number of cases like complex crystals, amorphous materials, liquid crystals, foams, and even biological organizations, with scales ranging from the atomic level up to macroscopic scales. In this paper, we discuss the close sphere packing problem, which has some relevance to the structural problem in amorphous metals, quasicrystals and some periodic complex metallic structures. The role of sets of disclination line defects is addressed, in particular with comparison with the major skeleton occurring in complex large-cell metals (Frank–Kasper phases). An interesting example of 12-fold symmetric quasiperiodic Frank–Kasper phase, and its disclination network, is also described.

RÉSUMÉ

La frustration géométrique apparaît lorsqu'une configuration préférentielle (par exemple de plus basse énergie pour des systèmes atomiques ou de compacité maximale dans les modèles sphères dures) ne peut se propager dans l'espace sans engendrer de défauts. Une approche générale a été proposée dès les années 1980, basée sur des modèles non frustrés définis dans des espaces courbes et qui permet d'analyser de nombreux cas, comme les intermétalliques complexes, les matériaux amorphes, les cristaux liquides, les mousses et même certains édifices biologiques dans une vision multi-échelle allant du niveau atomique au niveau macroscopique. Nous discutons dans cet article le problème de l'empilement de sphères en connexion avec le problème structural des amorphes métalliques, quasicristaux et intermétalliques complexes. On s'intéressera ensuite au rôle des ensembles de disinclinaisons, dont ceux rencontrés dans les grandes mailles des composés métalliques complexes comme les phases de Frank–Kasper. On décrira enfin un exemple intéressant d'une phase de symétrie locale dodécagonale quasipériodique de type Frank–Kasper, avec son réseau de disinclinaisons.

E-mail addresses: remy.mosseri@upmc.fr (R. Mosseri), sadoc@u-psud.fr (J.-F. Sadoc).

1631-0705/$ – see front matter
http://dx.doi.org/10.1016/j.crhy.2013.09.006

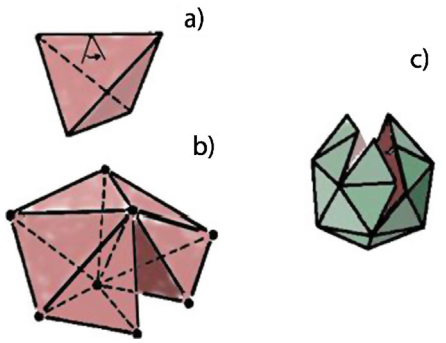

Fig. 1. Geometrical frustration for close tetrahedral packing in R^3. (Colour online.)

1. Introduction

Geometrical frustration appears in different contexts like complex crystals, amorphous materials, liquid crystals, foams and even biological organizations, with scales ranging from the atomic level up to macroscopic scales. It is generically encountered whenever a local configuration, which minimizes energy, cannot be freely propagated throughout space, leading to complex organizations. In this paper, we first recall the curved space approach, whose first step consists in curving the underlying space (here going to the three-dimensional sphere S^3) to release frustration. The real Euclidean structure is then analyzed, along the decurving procedure to R^3, in terms of ordered regions (close to that occurring in S^3), interrupted by topological defects, whose presence and density is directly related to the change of curvature from the curved to the flat space.

We shall focus here on the sphere dense packing problem in three dimensions, in relation with polytetrahedral and icosahedral order. An ideal, unfrustrated, template, the polytope $\{3, 3, 5\}$, is described in Section 2, in particular with the help of the so-called Hopf fibration. Section 3 relates decurving modes of this curved space template in terms of topological defects called disclination lines. These lines can be sequentially entered in the polytope using the Hopf fibration, leading to a first set of slightly decurved polytopes. A method to fully map the polytope into flat space, the iterative flattening method, is recalled, leading to hierarchical structures, with interlaced disclination defects. Such lines are also identified in known large-cell metallic alloy phases called Frank–Kasper phases. A related 12-fold quasicrystalline Frank–Kasper phase is described, and its disclination network displayed. This paper ends by an analysis of coordination number and disclination lengths in polytetrahedral close packings.

2. Hard sphere packing, frustration and curved space template

2.1. Dense sphere packing and icosahedral order

Consider the a priori simple but eventually very different geometrical hard sphere and hard disks packing problem. In two dimensions, three disks densely pack in the form an equilateral triangle, a configuration easily extended throughout the plane in the form of a periodic triangular packing; local and global order are compatible; this is an unfrustrated case. In three dimensions, the local densest packing of four spheres is achieved by placing their centers at regular tetrahedron vertices. The geometric frustration reveals immediately that the three-dimensional Euclidean space cannot be filled completely by regular tetrahedra. Indeed, the tetrahedron dihedral angle is $\theta = \cos^{-1}(1/3)$, slightly less than $2\pi/5$, which leads to the conclusion that five tetrahedra can be arranged around a common edge, with some remaining extra room. The latter accumulates when trying to propagate such a polytetrahedral dense packing, leading to pseudo-icosahedral arrangements at medium range and eventually a disordered sphere packing (Fig. 1).

The misfit angle around one edge can be made vanishing by changing the curvature of the underlying space. In the present case, upon embedding in a 3-dimensional positively curved space, the hypersphere S^3, the tetrahedron dihedral angle increases, and eventually reaches the value $2\pi/5$, which allows a perfect propagation of polytetrahedral order on a hypershere S^3 of appropriate radius (here the tetrahedral edge times the golden ratio $\tau = (1 + \sqrt{5})/2$). One gets a regular structure, a polytope, called the "600-cell" or the $\{3, 3, 5\}$ polytope [1], providing a very dense sphere packing (filling factor $\sim$0.78, therefore surpassing the Euclidean case), which has been intensively studied as an ideal template in the context of amorphous and complex crystalline metals [2–11].

Let us recall Coxeter notation for regular polytopes. A regular polyhedron $\{p, q\}$ has q p-gonal faces around each vertex: $\{4, 3\}$ is a cube, $\{3, 3\}$ is a tetrahedron. A polytope $\{p, q, r\}$ has r $\{p, q\}$ polyhedra around each edge. The $\{3, 3, 5\}$ is a finite structure on S^3, comprising 120 vertices, 600 tetrahedral cells. Each edge shares five tetrahedral cells, and each site is surrounded by a perfect icosahedral first shell. This polytope has a very large symmetry group, of order 14 400, the square of the double icosahedral group Y in $SU(2)$.

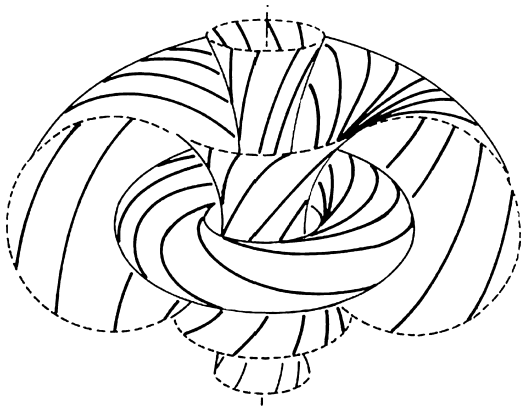

Fig. 2. A limited view of the S^3 Hopf fibration (stereographic map onto R^3).

2.2. Hopf map views of polytope $\{3, 3, 5\}$

Even though it can be embedded in a 4-dimensional space Euclidean space as $x_1^2 + x_2^2 + x_3^2 + x_4^2 = r^2$, one should not forget that the hypersphere S^3 is a (curved) 3-dimensional space (indeed, the four coordinates x_j are constrained by one equation). Let us have a closer look to S^3 via the concept of fibred space. A space has a fibre bundle structure if it contains a sub-space (the fibre) that can be reproduced by a displacement so that any point of the space is on a fibre and only one. For example, the Euclidean 3-space can be considered as a fibre bundle of parallel straight lines, all perpendicular to the same plane, or, dually, of parallel planes perpendicular to one line.

A fibred space E is defined by a mapping from E onto the so-called "base" B, any point of a given fibre F being mapped onto the same base point. A fibre is therefore the full pre-image of one base point under the mapping. A fibration is said to be trivial if the base space can be embedded in the full space, which leads to a simple product presentation $E = B \times F$. In the above simple R^3 example, the two-dimensional base space is just the plane orthogonal to fibres (or dually the line perpendicular to the planes). Said differently: $R^3 = R^2 \times R^1 = R^1 \times R^2$. But this latter property is not general, the simplest case being provided by the Hopf fibration [12] of S^3 by great circles S^1 and base S^2 for which $S^3 \neq S^2 \times S^1$.

The fibre is an S^3 great circle (parameterized by one angle) which map onto a point on the base S^2; the full inverse image of S^2 gives a fibration of S^3 with disjoint great circles, the Hopf fibration. A circle on the base S^2 corresponds to a torus in S^3, and the sequence of "parallel" circles on S^2 is an image of a torus foliation of S^3, of which three members are drawn in Fig. 2.

Looking to the base, a set of parallel circles on a sphere has three particular members: the (largest) equatorial circle and the two opposite poles, where the parallel circles degenerate into two points. The equatorial circle is the image, in the fibred sphere S^3, of the so-called "spherical torus", which has some interesting metrical properties and plays a role as a template for toroidal configurations in R^3, minimizing the Willmore functional [13]. Now, each such great circle in the fibration is surrounded by a toroidal neighbourhood, as illustrated for the central fibre in Fig. 2.

Back to the polytope case, it turns interesting to define discrete Hopf fibrations, as the set of fibres (associated with the symmetry axes of the polytope) that contain all the polytope vertices (Fig. 3). For the above polytope $\{3, 3, 5\}$, we are facing many different possibilities owing to the high order of the polytope symmetry group. Let us focus on the case where the circular fibres contain the largest number of polytopes sites, namely 10 arranged as regular decagons. The 120 sites of the polytope are then gathered along 12 fibres of ten sites. The nice point here is that the Hopf map sends the 12 fibres onto the 12 vertices of an icosahedron on the base S^2, which therefore gather information about the way these fibres are arranged in S^3. Two first neighbour points on the icosahedral base corresponds to two neighbouring fibres; the fact that one icosahedral vertex has five neighbours therefore images the symmetric arrangement of five fibres around a central one in the polytope. Finally, to a triangular face of the icosahedron corresponds a set of three fibres that realizes a compact pseudo-linear arrangement of tetrahedra very close to the well-known Boerdijk–Coxeter triple helix [14,15]. This discrete Hopf fibration will be used later to introduce disclination lines and decurve the polytope.

3. Frank–Kasper lines and disclinations

One can always, in an unambiguous way, connect a generic three-dimensional set of points, and get a (usually irregular) tetrahedral space division. This is done using first the Voronoï (or Dirichlet) decomposition of space into individual cells that contain the regions of space, closer to a given point than to any other one. In generic cases, the Voronoï cells have three faces sharing a vertex of the cell. Then, connecting the original points of the set whenever their associated Voronoï cells share a face defines a unique decomposition of the space into tetrahedra. This simplicial decomposition is equivalent, in three dimensions, to a point set triangulation in two dimensions. This procedure also provides a non-ambiguous way to define the coordination number in dense structure: it is the number of faces of the Voronoï cell. In a tetrahedral division

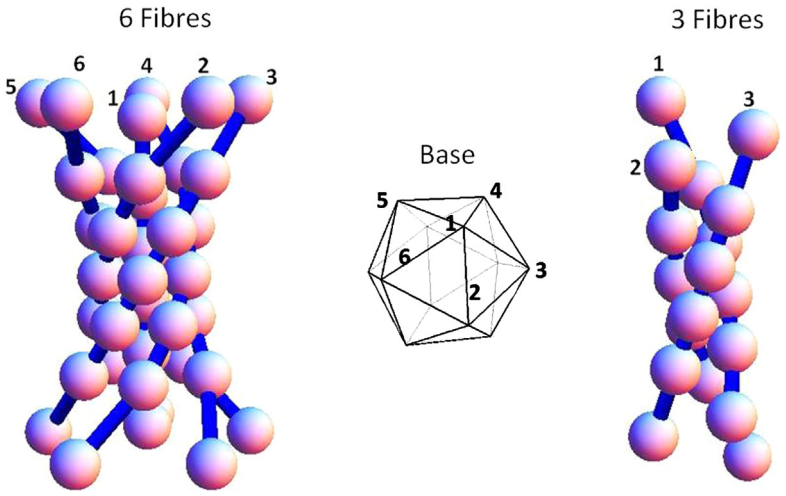

Fig. 3. Discrete Hopf fibration for polytope $\{3,3,5\}$. The Hopf fibration is oriented such that each fibre contains 10 sites. The base has 12 points with an icosahedral geometry. A finite portion of the polytope is stereographically mapped onto R^3, with the centre of projection along one central fibre, with its five neighbouring fibres (left); with the centre of projection located at the centre of a triangular face on the base (right), closely related to the Boerdijk–Coxeter triple helix. (Colour online.)

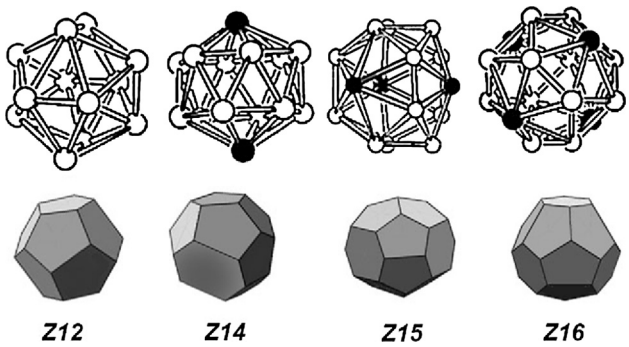

Fig. 4. Frank–Kasper polyhedra.

of space, the set of vertices closest to a given site forms its first coordination shell, which is a triangulated polyhedron (a deltahedron). Now, if the set of points is the centre of a compact sphere packing, the tetrahedral space division presents some regularities: a major part of the first coordination shells belong to a small set of deltahedra (called in some context the Frank–Kasper polyhedra), with interesting interconnections, which we now summarize.

3.1. Frank–Kasper polyhedra and phases

In their study of large-cell crystalline polytetrahedral structures, Frank and Kasper introduced a standard notation to distinguish atomic sites according to their coordination number [16,17]. If the tetrahedra are not too distorted, one mainly faces situations where either five or six tetrahedra share a given edge. A site whose first-neighbour shell is an icosahedron (allowing small distortions) is called a Z_{12} site. Additional sites are defined, denoted Z_{14}, Z_{15} and Z_{16} sites according to their numbers of neighbours (Fig. 4). Their corresponding coordination shells are deltahedra, with twelve 5-fold coordinated vertices and respectively two, three or four 6-fold coordinated vertices. It can be proved that these latter sites cannot occur isolated in the tetrahedrally divided space, but should form a subnetwork called the “major skeleton”. The edges of these networks are precisely those edges in the simplicial decomposition that share six tetrahedral cells. This topological property of Frank–Kasper structures is related to the non-existence of a canonical Z_{13} site together with the above requirement of having only five or six tetrahedra around each edge. We shall later identify this major skeleton with a disclination network. But let us first describe some large cell tetrahedrally close to packed crystalline phases.

These phases have been a main subject in metallurgical studies, with a pronounced renewed interest when it was realized that, in the large-cell case, they may occur as approximant phases for quasicrystalline alloys. These structures have been studied extensively by D. Shoemaker and C. Shoemaker [18], among others. They all show how a local tetrahedral arrangement can lead to periodic structures while keeping some icosahedral configurations. Let us describe the most common phases, with a focus on the different F–K polyhedra. The coordination number is now written at a upper place, in order to recover, as usual, the composition as an index (e.g., $Z_2^{(12)}$ means two Z_{12} sites in the unit cell).

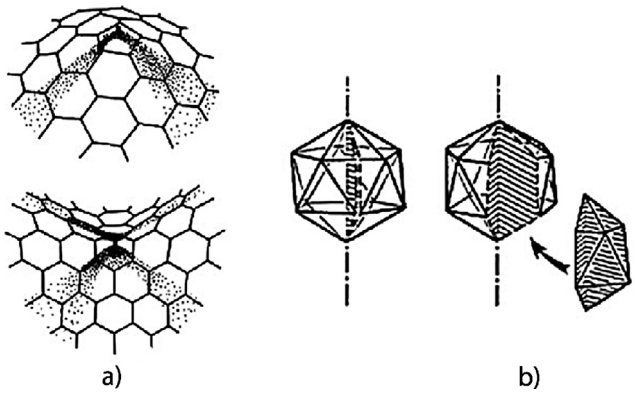

Fig. 5. Disclinations in 2d and 3d. (a) a disclination point at the centre of a hexagon change the size of a ring and concentrate curvature (positive or negative); (b) a $2\pi/5$ disclination line through an icosahedron transforms it into a Z_{14} site.

- $Z^{(12)}Z_3^{(14)}$ corresponds to the simplest examples of Frank–Kasper phases, the β phase of tungsten, also called the $A15$ structure. The $A15$ elementary cell is cubic and contains eight atoms. Inside the cube is a centered icosahedron, with the twelve outer atoms on the cube faces, which therefore count for 1/2. The eight cubic corners are also occupied (counting for 1/8). The three orthogonal 2-fold axes of the icosahedron coincide with the three 4-fold axes of the cube. Among the eight atoms of the elementary cell, two have an icosahedral coordination (Z_{12} sites) and six have a coordination polyhedron with 14 vertices (Z_{14} sites). These latter sites are connected along infinite straight lines (the major skeleton) running in the three spatial directions.
- $Z_2^{(12)}Z^{(16)}$ corresponds to Friauf–Laves phases, as for instance Cu_2Mg. They have a cubic cell with eight atoms of one type (Z_{16}-type, here Mg) and 16 atoms of a second type (Z_{12}-type, here Cu), filling the free space in the voids of the diamond structure. The coordination polyhedron for the former type of sites has 16 vertices (Z_{16} site) with the four six-fold coordinated vertices (arranged with tetrahedral symmetry) at the nodes of the diamond sub-structure. The latter type of sites have a slightly distorted icosahedral environment (Z_{12} sites). The structure of this cubic Laves phase can also be described as a stacking of sheets made of Friauf–Laves polyhedra and small tetrahedra (see below). All Cu atoms are on the vertices of these polyhedra, and the Mg atoms at their centre.
- A third encountered phase has the composition $Z_3^{(12)}Z_2^{(14)}Z_2^{(15)}$, corresponding to alloys such as Zr_4Al_3 (Zr on Z_{14} and Z_{15} positions).
- A last phase is interesting to mention in the present context: the $Mg_{32}(Zn, Al)_{49}$ crystalline alloy, known as the Bergman's structure [19] (also called T-phase), with its large cubic cell with 162 atoms and composition $Z_{49}^{(12)}Z_6^{(14)}Z_6^{(15)}Z_{20}^{(16)}$. Its great interest comes from its relation with approximants of quasicrystals of close composition. Notice that the sequence of the first three concentric polyhedra around a Z_{12} node of the cubic cell is an icosahedron of Z_{12} sites, a dodecahedron of Z_{16} sites and an icosahedron of Z_{12} sites. Up to this third shell, remarkably enough, this shelling is identical to that surrounding a $\{3, 3, 5\}$ vertex (but in the polytope, all sites are of type Z_{12}). We shall go back to this phase below.

3.2. Disclinations

A disclination is a defect involving a rotation operation, as opposed to the more familiar dislocation, which is associated with a translation given by it Burgers vector. A disclination can be generated by a so-called "Volterra" process, by cutting the structure along a surface ending on line and adding (or removing) a sector of material between the two lips of the cut [20,21]. In two dimensions, this defect is point-like, while it is linear in three dimensions. The two lips of the sector should be equivalent under a rotation belonging to the structure symmetry group in order to get a pure topological defect confined near the apex of the cut. It is possible to describe this defect, and the induced deformation, as a concentration of curvature (Fig. 5a). It is therefore natural to use disclination lines in order to map a positively curved space onto a flat one. We shall see that suitable disclinations can transform Z_{12} sites into the other Frank–Kasper polyhedra. One then expect that suitable disclination lines introduced in the polytope $\{3, 3, 5\}$ create structures containing a mixing of Frank–Kasper polyhedra.

In two dimensions, a disclination changes the coordination number when it goes through a vertex, or the size of a polygonal cell when the latter is threaded by the defect. In three dimensions, disclinations also change the network topology as exemplified in Fig. 5b, where a $2\pi/5$ disclination line through an icosahedron transforms it into a Z_{14} site. The central site and the two opposite vertices on the cut axis belong to the defect line. In a similar way, three halves (four halves) $2\pi/5$ disclination lines, meeting at the central vertex, transform a Z_{12} into a Z_{15} site (a Z_{16} site). It is possible to show that such lines cannot stop in the structure and either end at the surface, split at crossing points, or form closed lines. The set of crossing points and disclination segments or lines form a so-called disclination network. The Frank–Kasper major skeleton is

an instance of a disclination network in an icosahedral medium. So, introduction of disclinations not only allows decurving the embedding space, but it also generates slight modifications of the local configurations.

3.3. Disclinations in polytope $\{3,3,5\}$

3.3.1. Fibration approach

We now describe the effect of introducing two $2\pi/5$ disclination lines in the $\{3,3,5\}$ polytope. An elegant way to do that is to use the above discrete Hopf fibration [22]. As said above, polytope $\{3,3,5\}$ has twelve great circle fibres of ten sites that map onto the twelve vertices of an icosahedron. The fact that one fibre has five neighbouring fibres (Fig. 3, left) brings about (in the base) the fact that an icosahedral vertex has five neighbours. The idea is to select a pair of opposite great circles as the locus of line defects, and analyze the disclination procedure on the base. A disclination will change the number of edge-sharing tetrahedra along the defect line, changing the sites from Z_{12} to Z_{14}, with six, instead of five fibres around the "defect" fibre. As a result, the Hopf map of the disclinated structure will change from an icosahedron to precisely the 14-vertex polyhedron called Z_{14} (Fig. 4). In that case, the two black vertices in the figure are the Hopf map of the two disclination lines in S^3. This disclinated polytope has been called D_{14} [22]; it contains 168 sites, with 144 twelve-fold coordinated sites (Z_{12} sites) and 24 Z_{14} defective sites on the two opposite great circles. It is here interesting to recall the work of Straley [23], who studied, by numerical simulation, the ground state of 168 spheres on S^3, under a standard pair potential, and who obtained this same polytope, with the two same disclinations. It is further possible to consider Z_{15} and Z_{16} configurations on the fibration base, with three or four vertices having six neighbours. This leads to new disclinated polytopes with three and four disclination lines, having respectively 180 and 192 vertices that have been denoted D_{15} and D_{16}. Notice that an intrinsic limitation of this disclination procedure is that it introduces individual non-crossing defects lines along great circles. In order to go further and approach flattened structures with disclination networks, on needs to use another approach, the *iterative flattening method*, that we now describe.

3.3.2. Iterative flattening method

Instead of entering disclinations one by one, it is possible to generate sets of entangled disclination networks, leading rapidly to flattened structures. The proposed hierarchical flattening procedure [24,25] is based on an iterative decoration scheme, where a tetrahedrized structure is transformed into another tetrahedrized structure containing more tetrahedra and vertices. Consider a tetrahedral cell in the $\{3,3,5\}$ polytope and add two new vertices on each one of its edges, dividing them into three equal segments. The solid tetrahedron has been decomposed into four smaller tetrahedra and one truncated tetrahedron. This truncated tetrahedron is a ubiquitous structural unit observed in several metallic compounds, often called the Friauf–Laves (F.L.) polyhedron (see below). All the 600 $\{3,3,5\}$ cells are thus decorated, leading to a decomposition of the polytope into tetrahedral and F.L. cells. New vertices are then added at the centre of F.L. polyhedra (the centres of the original tetrahedral cells). Each hexagonal face of an F.L. polyhedron carries six tetrahedra (shared by two neighbouring F.L. polyhedra). Therefore, upon weighting the shared cells by one half, we see that a $\{3,3,5\}$ tetrahedral cell is decomposed into twenty smaller tetrahedral cells (Fig. 6a, b). One eventually finds three types of sites in this curved structure: (i) the 120 sites located at the $\{3,3,5\}$ vertices which remains Z_{12} sites; (ii) the 1440 added (by pairs) on each of the 720 $\{3,3,5\}$ edges, still of type Z_{12}; (iii) and finally the 600 sites added at the centre of the $\{3,3,5\}$ cell, which appear to be of Z_{16}-type. A disclination network has been generated, whose edges connect the centre of the $\{3,3,5\}$. This is nothing but the edges of the dual $\{5,3,3\}$ polytope, a regular packing of dodecahedral cells on S^3. This new tetrahedrally close-packed polytope, with 2160 sites, is denoted P_1 (with the $\{3,3,5\}$ as P_0).

Nothing prevents to apply this decoration again onto P_1, even though its tetrahedral cells are not regular, and gets a P_2 polytope, with a large number of Z_{12}, Z_{16} and also now Z_{14} sites. At each iteration, a scaling factor $\lambda = 3$ occurs between each interlaced disclination network. Upon iteration, the distribution of coordinations allows a simple algebraic description [24,25]. Let us form a three-dimensional vector $N_1^{(i)}$ with components (n_{12}, n_{14}, n_{16}), the number of Z_{12}, Z_{14} and Z_{16} sites at the ith iteration. The decoration procedure is encoded in a matrix Ω_1, such that $N_1^{(i)} = \Omega N_1^{(i-1)}$:

$$\Omega_1 = \begin{pmatrix} 13 & 12 & 12 \\ 0 & 3 & 4 \\ 5 & 6 & 8 \end{pmatrix}$$

The iteration begins with the $\{3,3,5\} = P_0$ and $N_1^{(0)} = (120,0,0)$. To the largest eigenvalue of Ω_1 (the so-called Perron root), here $\nu = 20$, corresponds an eigenvector whose components gives the average properties of P_∞. In particular, the mean coordination number, 40/3, is closely approached after only very few iterations. After p iterations, polytope P_p contains p interlaced disclination networks (Fig. 6c), which all share the $[3,3,5]$ symmetry group. As a consequence, these hierarchical structures display an orientational order, a point that appears clearly when looking at the optical Fourier transform of large clusters, mapped onto a tangent R^3 after several iterations [11].

3.4. Hierarchical decoration on Frank–Kasper phases

The above decoration applies to any tetrahedral close-packed structure, and therefore also to Frank–Kasper phases in R^3, leading to interesting structures. As an example, we have described a hypothetical structure, hereafter referred to as *S.M.*,

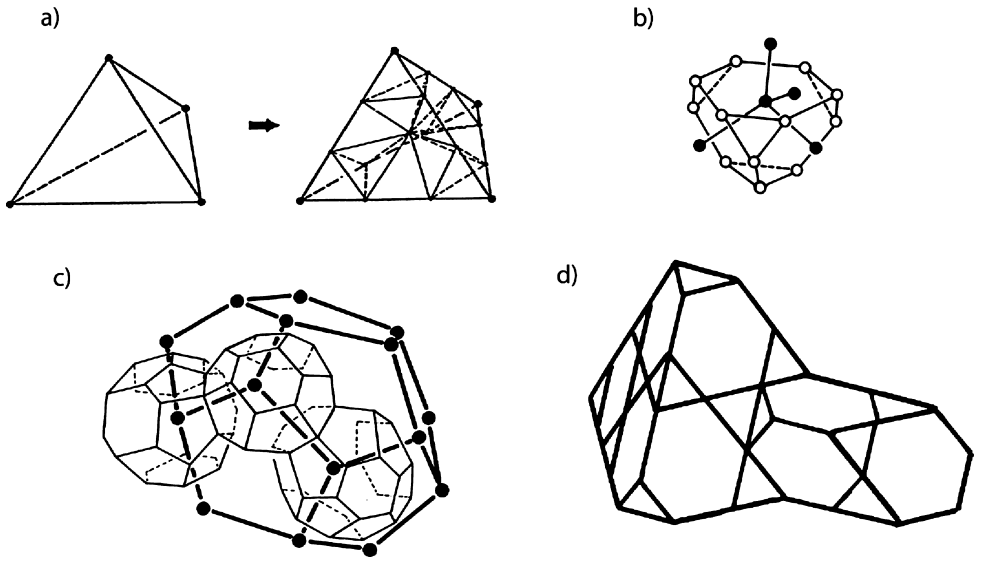

Fig. 6. Iterative flattening method and Friauf–Laves decoration. (a) Decoration procedure inside a tetrahedron; (b) Friauf–Laves polyhedron with one central (Z_{16}) site and its four disclination lines pointing at tetrahedral directions; (c) local view of the entangled disclination network after two iterations (polytope P_2); (d) packing of F.L. polyhedra in standard Friauf–Laves phases. Their centres form a diamond structure.

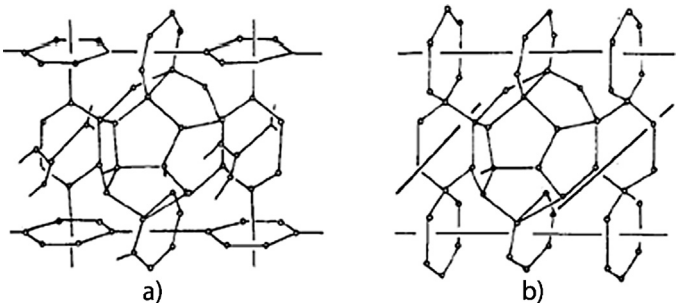

Fig. 7. Disclination network in the two related Bergman (a) and SM (b) phases; both present dodecahedral shells with Z_{16} sites.

corresponding to the application of the above Friauf–Laves decoration onto the $A15$ structure. Its formula is $Z_{49}^{(12)} Z_9^{(14)} Z_{23}^{(16)}$, as can be simply checked from the matrix Ω applied to vector $(1, 3, 0)$ which represents the $Z^{(12)} Z_3^{(14)}$ composition for $A15$. A remarkable fact is that this decorated structure is a simple variant of the above-mentioned Bergman (T) structure $Mg_{32}(Zn, Al)_{49}$, whose composition reads $Z_{49}^{(12)} Z_6^{(14)} Z_6^{15} Z_{20}^{(16)}$. *S.M.* and T phases (which share the same mean coordination number $\bar{z} \simeq 13.358$) are both cubic structures with similar coordination shells around vertices and center of the cubic cell; they only differ in the orientation of these shells: they are similar with regard to the T phase, which is therefore body-centered cubic, while different for the *S.M.* structure, which has therefore a simple cubic symmetry (inherited from the $A15$). Notice in Fig. 7 their main difference: in addition to the Z_{12}, Z_{14} and Z_{16} sites common to both structures, the Bergman phase contains Z_{15} sites (three-fold coordinated sites in the disclination network). The above decoration can be applied to any F–K phase, and even iterated as for the polytope. This would lead to an infinite family of large-cell tetrahedrally close-packed structures with entangled disclination networks, whose relation with quasicrystals is an interesting open question. But another route to quasiperiodic structures is explored in the following section.

3.5. A 12-fold symmetric quasiperiodic Frank–Kasper-like phase

Up to now, we have described the F–K phases in terms of their major skeleton. It is also interesting to recall their analysis in terms of their possible planar sub-structures. In their original papers, Frank and Kasper described a large set of tetrahedrally close-packed structures in terms of main layers tiled by triangles with hexagons or pentagons, supplemented in between by secondary (less dense) layers tiled by square (or rectangles) and triangles [16,17,26]. We consider here only those structures whose main layers contain triangles and hexagons, and focus on their intermediate layers geometry. Indeed, it is possible to define a local atomic decoration with respect to such triangle-square tilings, which eventually leads to the full set of atomic positions, once periodically repeated in the orthogonal direction. These structures contain Z_{12}, Z_{14}, and Z_{15} sites, and interestingly simple disclination networks. A nice example is provided by the σ phase: the disclination network is

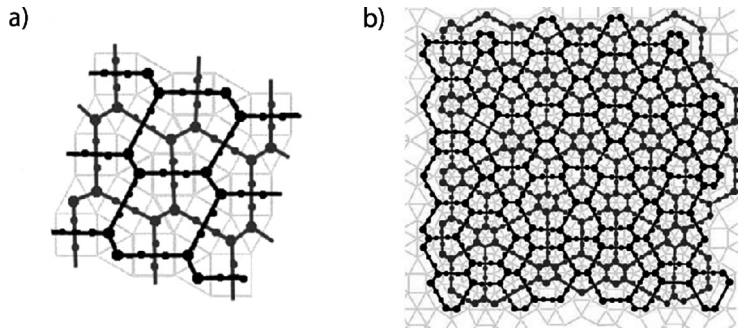

Fig. 8. Disclination networks for (a) the σ phase and (b) the 12-fold quasicrystal. Both are constructed as periodically spaced parallel layers with hexagonal packings having the Z_{15} sites at the nodes (large disks) and the Z_{14} sites along the edges (smaller disks). The σ phase network has one type of periodically repeated (non-regular) hexagons, with two different orientations according to the layer. The quasicrystal shows a quasiperiodic tiling of several types of hexagons, with again two different orientations according to the layer.

made of stacked layers, with Z_{15} sites at the centres of triangles and Z_{14} sites in between, arranged in (irregular) hexagonal tilings that alternate in orientation (Fig. 8a). Now there are already plenty of different periodic, disordered, and even a quasiperiodic 12-fold symmetric patterns, which differ by the ratio of squares and triangle, and their relative arrangement. We shall not present here the detailed atomic decoration, but rather give the correspondence between the ratio of squares to triangles and the relative frequency of different types of sites.

Let us form a two-dimensional vector $\mathcal{V}$ with components $(n_\mathrm{s}, n_\mathrm{t})$, the number of squares and triangles (which can be given in terms of relative frequencies for infinite structures), and a three-dimensional vector N_2 with components (n_{12}, n_{14}, n_{15}), the number of Z_{12}, Z_{14} and Z_{15} atomic sites upon decoration. The atomic decoration, once coded as a relation between $\mathcal{V}$ and N_2, takes the simple (rectangular) matrix form:

$$N_2 = \begin{pmatrix} 2 & 3/2 \\ 6 & 1 \\ 0 & 1 \end{pmatrix} \mathcal{V}$$

With $y = n_\mathrm{s}/n_\mathrm{t}$, the average coordination number for the decorated structures reads:

$$\bar{z} = \frac{108y + 47}{8y + 7/2}$$

This describes a large and interesting set of Frank–Kasper phases. The $A15$ phase has only squares in the intermediate layer (therefore infinite y), which leads to $\bar{z} = 13.5$. The Z phase has only triangles ($y = 0$), leading to $\bar{z} \sim 13.429$. And the above σ phase corresponds to $y = 1/2$, leading to $\bar{z} \sim 13.467$.

An interesting member of the triangle-square tilings is provided by the quasiperiodic dodecagonal tiling, which was popularized when 12-fold quasicrystals were discovered [27], showing an interesting case with symmetry differing from that of the icosahedral quasicrystal [28]. These tilings allow an inflation–deflation construction that is summarized by the following transfer matrix relating $\mathcal{V}^{i+1}$ to $\mathcal{V}^{i}$ between two consecutive generations:

$$\mathcal{V}^{(i+1)} = \begin{pmatrix} 7 & 3 \\ 16 & 7 \end{pmatrix} \mathcal{V}^{(i)}$$

To this matrix of largest eigenvalue $7 + 4\sqrt{3}$ corresponds an eigenvector $\{\sqrt{3}/4, 1\}$ giving the asymptotic (for the quasiperiodic structure) relative frequency between squares and triangles. It is then easy to get the average coordination $\bar{z} \sim 13.464$, and even the (unnormalized) composition $Z_r^{(12)} Z_s^{(14)} Z_t^{15}$, with $r = 3 + \sqrt{3}$, $s = 2 + 3\sqrt{3}$ and $t = 2$. It is interesting to have a look to the disclination network (Fig. 8b), and compare it, for example, to that of the σ phase. As expected, the disclination network is itself quasiperiodic, made of hexagons of different shapes.

3.6. Coordination number and disclination lengths in tetrahedrally close-packed structures

It is well known that, in two dimensions, tilings are subject to constraints leading to conserved quantities depending on the underlying space curvature and topology [11]. From the mathematical point of view, this results from applying Gauss–Bonnet and Euler–Poincaré relations, which leads to interesting sum rules on the proportions of ring sizes or coordination numbers. As an example, one easily derives that for any c-fold coordinated (c being constant) tiling on a domain $\mathcal{D}$ of a curved manifold (with Gaussian curvature κ, not necessarily constant), the following relation applies for F_p, the number of p-gonal faces:

$$\sum_{p=3}^{\infty} (2c - cp + 2p) F_p = \frac{c}{\pi} \iint_{\mathcal{D}} \kappa \, \mathrm{d}\sigma$$

The symmetry between c and p allows us to treat the dual problem with constant p-gonal faces and varying coordinations. One than get, with a vanishing right-hand side, the known fact that for any triangulated two-dimensional flat structure, the average coordination number is six. Notice that whenever $(2c - cp + 2p) = 0$, the corresponding F_p does not contribute to the sum rule, leading to the concept of *neutral charge* polygons. As said above, disclinations in two dimensions are point-like defects, carrying curvature, and their main effect is to change the ring size or the coordination number in a tiling. The above sum rule can therefore result in disclination distributions, with the concept of *deficit angle* carried by a disclination. Let us first recall how the area of a 2-dimensional sphere S^2 can be faithfully computed by summing over angular deficits at the vertices of a discretized structure, a polyhedron, covering this surface. The surface is considered as being flat everywhere, except on the (regular) polyhedron $\{p, q\}$ vertices that concentrate curvature. The angular deficit δ of each vertex is $\delta = 2\pi - q\alpha_p$ where α_p is the vertex angle of a p-gonal face. So, $\delta = \pi[4 - (p-2)(q-2)]/p$. The number of vertices V in a regular polyhedron $\{p, q\}$ is easily deduced from the Euler relation, as $V = 4p/[4 - (p-2)(q-2)]$. Consequently, the total angular deficit for a polyhedron is $\sum \delta = 4\pi$, precisely the area of a unit radius sphere S^2.

The three-dimensional case is less constrained and do not lead to simple unique value, but rather to ranges of expected values. For tetrahedrally close-packed structures, one can focus on two related quantities, the mean coordination $\bar{z}$ and the mean number of tetrahedra sharing an edge $\bar{r}$. For the regular $\{3, 3, 5\}$ polytope, one has trivially $\bar{z} = 12$ and $\bar{r} = 5$. Disclination lines affect these values, which increase when going from a positively curved space to a flat space. In flat space, most structures of interest (with slightly distorted tetrahedral cells) have $\bar{r} \sim 5.1$ and $\bar{z}$ in the range 13.3–13.5. A nice mean-field-like approach to this packing problem in three dimensions is provided by the Coxeter statistical honeycomb [29]: using the above given regular tetrahedron dihedral angle θ, one expects an average of $\bar{r} = 2\pi/\theta \simeq 5.1043$ tetrahedra sharing an edge, forming the average structure $\{3, 3, \bar{r}\}$. Consider the average Voronoï cell surrounding one vertex: it is generically a polyhedron with 3-fold coordinated vertices, which can be viewed as a tiling on a closed surface equivalent to a sphere. The above relation leads to $\sum_p (6-p)F_p = 12$; introducing the face mean size $\bar{p} = (\sum pF_p)/F$ and assuming (the main approximation here) that the Voronoï cells are all equivalent, one gets $\bar{F} = 12/(6 - \bar{p})$. With the above $\bar{r}$, one finds $\overline{F}$ for the Voronoï cell, and therefore the average coordination $\bar{z} \sim 13.3973$, well in the middle of the observed range for compact tetrahedral packing.

It is then possible to go further in the analysis, and get an approximate sum rule, by considering the flat tetrahedral packing as having an underlying corrugated geometry [30] (with alternation of positive and negative curvature), and applying Regge-like analysis [31], which focuses on the deficit angle carried by disclination defects; in a similar way, Regge's calculus uses a simplicial decomposition of a curved manifold. The space enclosed by a tetrahedron is regarded as flat and the curvature is concentrated on the edges. When r tetrahedra share an edge, the angular deficit reads $\delta_r = 2\pi - r\theta$. The quantity δ_5 ($\simeq$01283 rad) is positive, corresponding to a positively curved space (similar to polytope $\{3, 3, 5\}$), while δ_6 ($\simeq -1.102$ rad) is negative (corresponding to a hyperbolic negatively curved space H^3). Consider a tetrahedrally close-packed structure, and suppose that one has only five or six tetrahedra sharing edges (like in Frank–Kasper phases). Such a network is now viewed as a Regge skeleton whose edges code an underlying curved topology, flat on the average, with the 5-fold (resp. 6-fold) edges in the positively (resp. negatively) curved regions. One shows that the requirement of vanishing curvature reads: $L_5\delta_5 + L_6\delta_6 \simeq 0$, where L_5 and L_6 are the lengths per unit volume of edges sharing five or six tetrahedra. Notice that, if necessary, this sum rule can be generalized to cases with other numbers of edge-sharing tetrahedra.

Let us carry out a simple calculation in the case of the hierarchical polytope where we assume for simplicity that all first-neighbour distances are equal. Then, in polytope P_i, each disclination edge carries a negative weight δ_6, while the other polytope edges carry a positive weight δ_5. Let us introduce the ratio $\Delta = L_5/L_6$. If the above relation were exact, then one expects $\Delta = \delta_5/|\delta_6| = 8.589$, for the fully flattened polytope P_∞. For the iterative polytopes P_i, $\Delta^{(i)}$ reads out from the knowledge of the respective triplet (n_{12}, n_{14}, n_{16}) as $\Delta^{(i)} = 6(n_{12}^{(i)} + n_{14}^{(i)} + n_{16}^{(i)})/(n_{14}^{(i)} + 2n_{16}^{(i)})$. At the infinite limit, one finds $\Delta^{(\infty)} = 9$, which is rather close to the above ideal value.

Being in a situation where no exact results exists, but apparent tendencies are present, we find it interesting to display some data in the following way. We focus on those close-packed structure that only contains Z_{12}, Z_{14}, Z_{15} and Z_{16}, and use their proportions (p_{12}, p_{14}, p_{15}, p_{16}) as barycentric coordinates (Fig. 9) inside a tetrahedron whose vertices correspond to regular configurations with only one type of site. The set of structures sharing the Coxeter statistical honeycomb mean coordination would lie on a plane, shown in the figure. Also displayed are several Frank–Kasper phases, polytope $\{3, 3, 5\}$ and the hierarchical polytopes described in the text, all falling in the vicinity of the mean-field plane. This plane separates ranges of parameters describing positively and negatively curved space structures.

4. Conclusion

In this paper, we have gathered some geometrical ingredients that allow a generic description of close-packed tetrahedral structures, related to icosahedral order at different scales. At a local scale, sphere packing and associated polytetrahedral close packing are known to lead to a pseudo-icosahedral local order, whose presence is expected in amorphous metals and undercooled metallic liquids. The extent to which a perfect local icosahedral order can be propagated is limited by frustration and leads to the presence of an intrinsic set of disclination defect lines. A disordered disclination network would lead to an amorphous structure, while such a periodic network corresponds to large-cell Frank–Kasper phases (some of which are found among quasicrystal approximants). A simple example of a 12-fold quasiperiodic Frank–Kasper phase is also

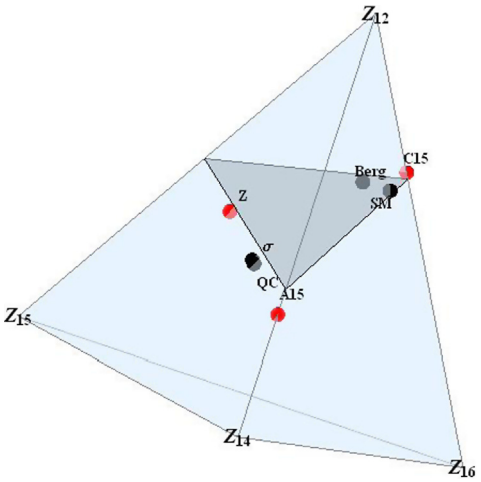

Fig. 9. Location of different phases depending on their ratio of four possible Frank–Kasper coordinations (Z_{12}, Z_{14}, Z_{15}, and Z_{16}), using barycentric coordinates. The dark plane corresponds to the mean coordination number of the Coxeter statistical honeycomb. Polytope $\{3, 3, 5\}$ sits at the Z_{12} vertex. The plane vicinity contains Euclidean structures, separating positively and negatively curved structures. Notice the $A15$, Z, σ and quasicrystalline (QC) phases, which are, as expected, in the (Z_{12}, Z_{14}, Z_{15}) plane. (Colour online.)

described here, with its quasiperiod layered disclination network. A final possibility, discussed here, is that of a hierarchical disclination network (entangling many scales), which is exemplified by the hierarchical polytopes. In all cases, a main geometrical description tool is provided by the ubiquitous Frank–Kasper polyhedra.

References

[1] H.S.M. Coxeter, Regular Polytopes, Dover Publications, Inc., 1973.
[2] M. Kleman, J.-F. Sadoc, J. Phys. Lett. 40 (1979) L569.
[3] J.-F. Sadoc, J. Non-Cryst. Solids 44 (1981) 1.
[4] J.-F. Sadoc, R. Mosseri, J. Phys. C 4 (42) (1981) 189–192.
[5] J.-F. Sadoc, R. Mosseri, Philos. Mag. B 45 (1982) 467–483.
[6] D. Nelson, Phys. Rev. Lett. 50 (1983) 982; Phys. Rev. B 28 (1983) 5515.
[7] J.-F. Sadoc, R. Mosseri, J. Non-Cryst. Solids 61–62 (1984) 487.
[8] D. DiVincenzo, R. Mosseri, M.H. Brodsky, J.-F. Sadoc, Phys. Rev. B 29 (1984) 5934.
[9] R. Mosseri, D.P. DiVincenzo, J.-F. Sadoc, M.H. Brodsky, Phys. Rev. B 32 (1985) 3974–4000.
[10] R. Mosseri, J.-F. Sadoc, Curved space model of amorphous semiconductors, J. Non-Cryst. Solids 77–78 (1985) 179–190.
[11] J.-F. Sadoc, R. Mosseri (Eds.), Geometrical Frustration, Cambridge University Press, 1999.
[12] H. Hopf, Mathematische Annalen, vol. 104, Springer, Berlin, 1931, pp. 637–665.
[13] R. Mosseri, J.-F. Sadoc, J. Charvolin, in: R. Lipowski, D. Richter, K. Kremer (Eds.), The Structure and Conformation and Amphiphilic Membranes, in: Springer Proceedings in Physics, vol. 66, 1992.
[14] A.H. Boerdijk, Philips Res. Rep. 7 (1952) 303.
[15] H.S.M. Coxeter, Can. Math. Bull. 28 (1985) 385.
[16] F.C. Frank, J.S. Kasper, Acta Crystallogr. 11 (1958) 184.
[17] F.C. Frank, J.S. Kasper, Acta Crystallogr. 12 (1959) 483.
[18] C.B. Schoemaker, D.P. Schoemaker, in: M. Jaric, D. Gratias (Eds.), Aperiodicity and Order, vol. III: Extended Icosahedral Structures, Academic Press, 1989.
[19] G. Bergman, J.L.T. Waugh, L. Pauling, Acta Crystallogr. B 42 (1957) 254.
[20] M. Kleman, Points, lignes et parois, Éditions de Physique, 1977.
[21] M. Kleman, Points, Lines and Walls, John Wiley, 1983.
[22] S. Nicolis, R. Mosseri, J.-F. Sadoc, Europhys. Lett. 1 (1986) 571.
[23] J.-P. Straley, Mater. Sci. Forum 4 (1985) 93.
[24] R. Mosseri, J.-F. Sadoc, J. Phys. Lett. 45 (1984) L827–L832.
[25] J.-F. Sadoc, R. Mosseri, J. Phys. 46 (1985) 1809–1826.
[26] J.M. Sullivan, in: N. Rivier, J.-F. Sadoc (Eds.), Foams and Emulsions, in: NATO Advanced Science Institute, Series E: Applied Sciences, vol. 354, Kluwer, 1998, pp. 379–402, or Proc. Eurofoam, Delft, The Netherlands, 2000, pp. 111–119.
[27] T. Ishimasa, H.-U. Nissen, Y. Fukano, Phys. Rev. Lett. 55 (1985) 511.
[28] D. Shechtman, I. Blech, D. Gratias, J.W. Cahn, Phys. Rev. Lett. 53 (1984) 1951.
[29] H.S.M. Coxeter, Ill. J. Math. 2 (1958) 746.
[30] R. Mosseri, J.-P. Gaspard, J. Non-Cryst. Solids 97–98 (1987) 415–418.
[31] J.-F. Sadoc, R. Mosseri, J. Phys. 45 (1984) 1025.